Al-Rafidain Engineering Journal (AREJ) Vol. 29, No. 1, March 2024, pp. 126-131

Design and Miniaturized a High Suppression Stop band Microstrip Low Pass Filter by using Slot Defected Ground Structure for 5G Applications

Ashraf Khalid Azeez Al-Hussein
ashraf.21enp13@student.uomosul.edu.iq

Saad Wasmi Osman Luhaib
s.w.o.luhaib @uomosul.edu.iq

Electrical Engineering Department, College of Engineering, University of Mosul, Mosul, Iraq

Received: December 11th, 2023 Received in revised form: January 30th, 2024 Accepted: February 18th, 2024

ABSTRACT

In this paper, a low-pass filter (LPF) microstrip generalized Chebyshev type defected ground with a high suppression stopband was proposed. The resonators of the suggested filter were implemented using a T-shape microstrip. The filter resonators consist of three main parts. A part of the resonators was used to improve the rejection of the filter in the stopping region, a second part was used to increase the selectivity of the filter, and the last part was used to balance between the two regions. The microstrip LPF filter is designed on a Roger RT/Duroid 5880 substrate with εr=2.2, a thickness of 0.381 mm. 11th order generalized Chebyshev LPF was simulated using HFSS software. The simulation results were as follows: 2 GHz for the cut-off frequency, insertion loss of 0.55 dB at about 20 dB return loss, and a wide range of stopband suppression below the level of 28 dB from frequency 3.4 GHz to 20 GHz. The LPF selectivity was approximately 37.5 dB/GHz and a small and compact size filter with 0.014λ2g was introduced. The filter matches the specifications required for fifth-generation filters in wireless communications systems.

Keywords:

Low pass filter; Microstrip; High suppression; Defected ground structure; DGS.

This is an open access article under the CC BY 4.0 license (http://creativecommons.org/licenses/by/4.0/).
https://rengj.mosuljournals.com
Email: alrafidain_engjournal1@uomosul.edu.iq

==========

1. INTRODUCTION

Low pass filters (LPF) are considered one of the important elements in all communication systems, especially after the development in the field of communications and the need for a high data rate and small size[1] . Furthermore, they are used to remove the spurious harmonics produced by the filters used in communications systems due to the repetitive effect of transmission lines. This will allow the frequencies of other systems to interface with the fundamental frequency[2]. There are many types of low-pass filters depending on their realization, such as microstrip , strip line , waveguide , coaxial , dielectric , suspended microstrip and lumped element[3]. The most famous type is the microstrip because it is easy in fabrication process , small size and low costs[4] . In [5] the proposed microstrip LPF consists of equally spaced parallel transmission lines, a patch with a cross configuration, and an adjusted E-shape feed structure. This filter exhibits a small overall footprint, a high roll-off characteristic, and a wide stopband. However, the signal suppression level in the stopband is about 15 dB. A new LPF based on microstrip technology is introduced, featuring a compact design. The filter incorporates a pair of patches balanced capacitors positioned on the top of the substrate layer and a DGS resonator in the ground of the substrate that provides sharp roll-off, but the stopband is just from 3.5 GHz up to 11.5 GHz [6]. A LPF was designed to involve a stepped impedance line in the upper layer of the substrate compact with an unbalanced π-shape in the ground plane. The filter offers a small size and sharp roll-off but the signal suppression level is more than 15 dB and the rejecition band is less than 10 GHz [7]. A compact LPF has been implemented by incorporating open stubs, a spurline resonator on the front layer, and enhanced DGS in the microstrip. The filter has achieved a very sharp roll-off rate and a good rejection band , but its suppression level was just 18dB and the size was

also not good[8] . In [9] the design incorporates two open resonators (ORs) in a rectangular shape, with multiple segments of the inter digital capacitor loaded on to them, it is had sharp roll-off attenuation band is good , but it is complex design methodologies, and the size is not quite good .

This paper will study and design a microstrip generalized Chebyshev DGS low pass filter with a small and compact size to present a wide rejection stopband and high spurious window that are used in 5G communication systems. The simulations were performed by a HFSS software and the microstrip substrate is Roger RT/Duroid 5880 with ε_r=2.2, thickness of 0.381 mm and tanδ=0.0009.

2. FILTER DESIGN

The proposed LPF introduces as lumped element (LC) is shown in Fig. (1). It has three parts of resonators , and each part of the design has characteristics that are necessary . The first part operates at high frequency to provide a high suppression band at the periodic harmonic, which occurred because of the transmission line theory. The second part of the parts responsible for transmission zero (TZ) frequency is designed to work at frequencies close to the conduction band. In order to provide a sharp roll-off and minimize the order of the filter, the final part will balance between the high and low transmission zeros , because without this part, the response rejection value will decrease significantly . To achieve the resonator of TZ in microstrip topology , T-shaped resonators are utilized and the inductance is used as strip of transmission line. A generalized Chebyshev low pass filter was designed for 5G applications, and the required specifications were as follows: $f_C = 2\ GHz$, $Insertion\ loss(IL) = 0.1\ dB$, $TZ_1 = 12\ GHz$, $TZ_2 = 3.5\ GHz$, $TZ_3 = 9\ GHz$. To calculate the values of inductances and capacitors in figure (1), the Newton–Raphson method was used to solve the equation (1) [10][11] .

$$F_N = \frac{j}{2}\left(\left\{\prod_{r=1}^{N}\frac{1+pp_r+[(1+p^2)(1+p_r{}^2)]}{p-p_r}\right\}+\prod_{r=1}^{N}\left\{\frac{1+pp_r-[(1+p^2)(1+p_r{}^2)]}{p-p_r}\right\}\right) \quad \ldots\ldots (1)$$

To convert from LC circuit to microstrip will use the following equations (2) to (4) [12]

$$l_L = \frac{\lambda_{gL}}{2\pi}\sin^{-1}\left(\frac{\omega_C L}{Z_{OL}}\right)$$

$$l_C = \frac{\lambda_{gC}}{2\pi}\sin^{-1}(\omega_C C\ Z_{OC}) \quad \ldots\ldots (2)$$

where λ_{gL} and λ_{gC} are the related guided wavelength, Z_{OL} and Z_{OC} are the impedance of transmission lines which are reperented the inductance and capacitance in LPF LC prototype respectively.

The effective dielectric constant for the transmission line is given by [12]:

$$\varepsilon_{re} = \frac{\varepsilon_r+1}{2} + \frac{\varepsilon_r-1}{2}\left(1+12\frac{h}{w}\right)^{-0.5} \quad \ldots\ldots (3)$$

where $\frac{h}{w}$ is the height to width ratio of the substrate. The guided wavelength can be evaluated directly in millimeters as follows [12]:

$$\lambda_g = \frac{300}{f(GHz)\sqrt{\varepsilon_{re}}}mm \quad \ldots\ldots (4)$$

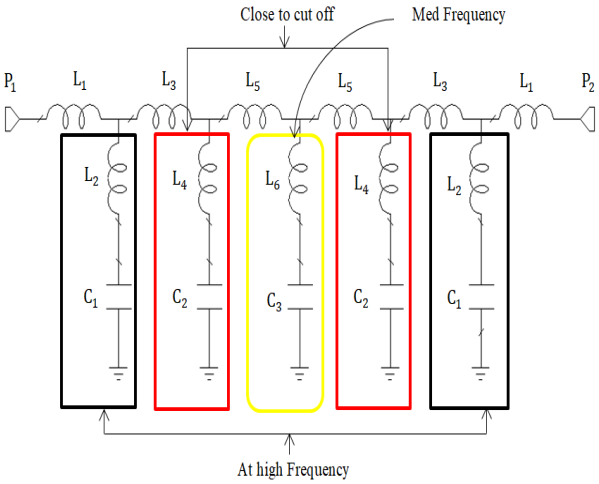

Fig. 1 LC equivalent circuit of 11th generalized Chebyshev LPF.

3. RESULTS AND DISCUSSIONS

To ensure the proper operation of each of the three parts of the TZs in Fig.(1), a simulation is performed for each part separately.

Figure 2(a) shows the layout of the microstrip and the frequency response for the high TZ. The position of high TZ was chosen to be 12 GHz, which is far away from the cutoff frequency. The result in Fig3 (b) shows that two TZs are at 12 GHz, while the other TZ is at 14 GHz which comes from the periodically resonant frequency for the transmission line theory. The passband response is not fit with the requirement of the filter because the all resonant does not account in this case.

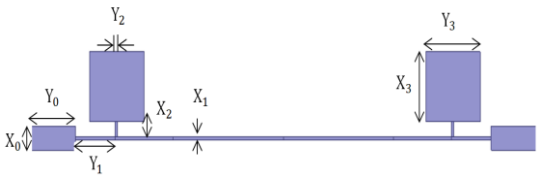

(a)

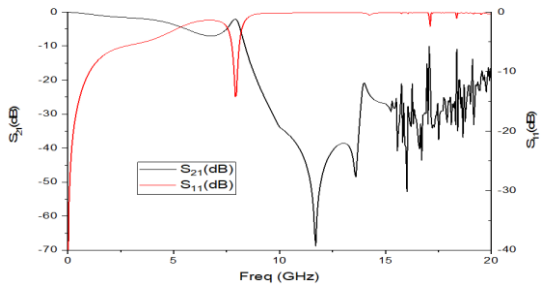

(b)

Fig. 2 (a) Top view of microstrip LPF with two high TZs (b) Simulation of frequency response of two high TZs.

Fig. (3) shows the top view of the microstrip, and the frequency response at the TZ location was designed to be closed to the pass band. The result shows that two transmission zero at a frequency of 3.5GHz.

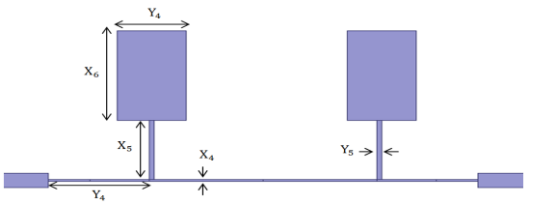

(a)

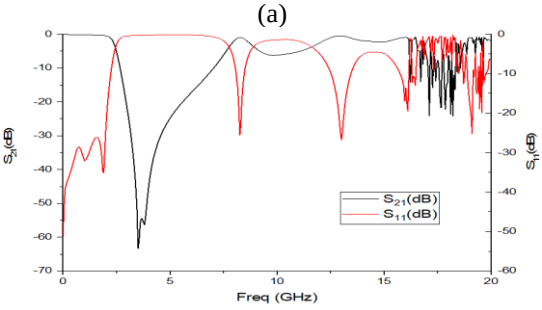

(b)

Fig. 3 (a) Top view of microstrip LPF with two TZs closed to passband(b) Simulation of the frequency response of two TZs closed to passband.

As mentioned previously, the third resonator works to balance the TZ locations that are close to the passband and that are far away. The Fig.(4) shows that the location of the transmission zero is at a frequency of about 9 GHz, which represents the organized region between TZs at 3.5GHz and 12GHz.

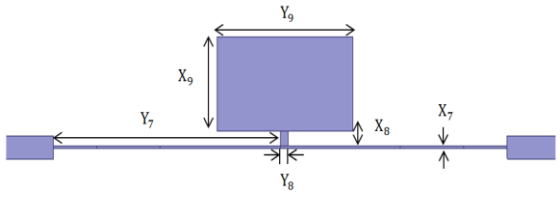

(a)

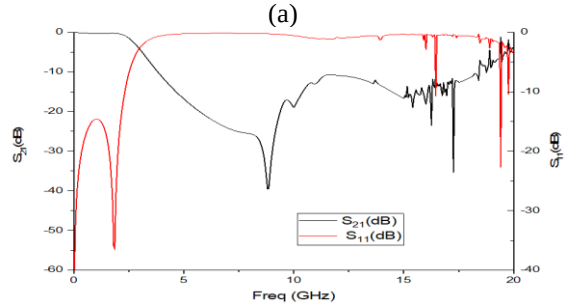

(b)

Fig. 4 (a) Top view of microstrip LPF with one TZ at miderate frequency (b) Simulation of the frequency response of one TZ at miderate frequency.

Fig. 5(a) presents final design of the microstrip LPF after combining the three parts together. The microstrip LPF impedances for all elements were chosen to be $Z_{OC} = 20\ \Omega$, $Z_{OL} = 150\ \Omega$ and the characteristic impedance is $50\ \Omega$. Table 1 illustrates the length of the physical dimensions of the LC LPF circuit, where all dimensions have been shown in table 2. Some values did not give the required response, for that optimization processes have been applied.

Table 1: Calculated and Optimized Physical lengths.

Value of elements	Calculated length	Optimized length
L1=1.72 nH	$l_L = 2 \quad mm$	$l_{Lo} = 1.8\ mm$
L2=0.48 nH	$l_L = 0.6\ mm$	$l_{Lo} = 0.5\ mm$
L3=2.1 nH	$l_L = 3 \quad mm$	$l_{Lo} = 2.6\ mm$
L4=4 nH	$l_L = 3.8\ mm$	$l_{Lo} = 3.3\ mm$
L5=5.2 nH	$l_L = 4.96\ mm$	*No change*
L6=0.4 nH	$l_L = 0.5\ mm$	*No change*
C1=0.33 pF	$l_C = 2.2\ mm$	$l_{Co} = 2.3\ mm$
C2=0.55 pF	$l_C = 4.8\ mm$	$l_{Co} = 5\ mm$
C3=0.74 pF	$l_C = 5.6\ mm$	*No change*

Table 2: The dimensions of the suggested LPF.

Parameter	Value (mm)	Parameter	Value (mm)
X_0	0.8	Y_0	2
X_1	0.1	Y_1	1.8
X_2	0.5	Y_2	0.1
X_3	2.3	Y_3	2.45
X_4	0.1	Y_4	2.6
X_5	3.3	Y_5	0.22
X_6	5	Y_6	3
X_7	0.1	Y_7	4.96
X_8	0.5	Y_8	0.33
X_9	3.24	Y_9	5.6

Fig.5(b) shows the wide frequency response of the 11th order generalized Chebyshev microstrip LPF. It notices that the cut-off frequency was 2GHz at a return loss(RL) of 12dB. The greatest insertion loss (IL) in the passband was 0.6 dB at frequency 1.4GHz, the difference between the designed and the simulation result of the IL value comes from losses in microstrip. It can also be seen that the filter provides a high roll-off is 37.5 (dB/GHz) and the locations of the TZs were distributed over the entire frequency response. The suppression level was less than 18dB for all the responses up to 20GHz.

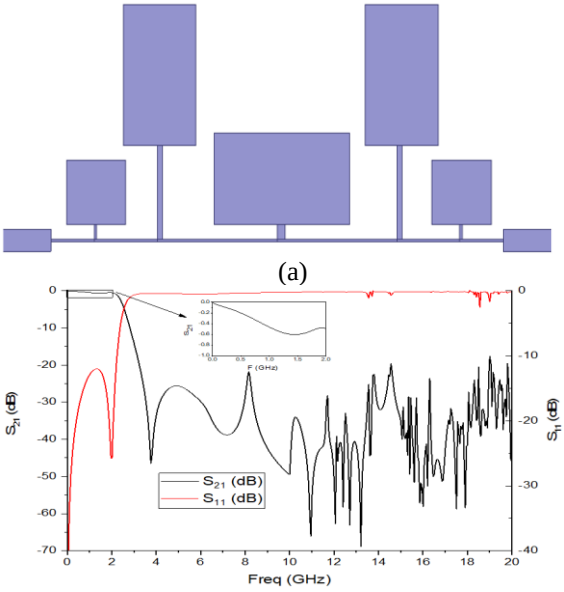

Fig. 5 (a) Top view of the 11th generalized Chebyshev microstrip LPF (b) Simulation of the frequency response of the 11th generalized Chebyshev microstrip LPF.

To improve the suppression level of the filter in the stopband region, a slot in DGS slot is used with these dimensions (width= 0.5 mm , length=2.7 mm) as shown in Fig. 6(a) . The results in Fig. 6(b) shows the suppression level is 28dB from 3.4 GHz to more than 20GHz, and the number of spicks has decreased because of the capacitive effect of the slot. There is an enhancement in the maximum IL in the passband of about 0.05dB compare to without DGS.

4. FILTER CHARACTERISTICS

The characteristics of the proposed generalize Chebyshev LPF with DGS can be identified using some standard equations (5)-(9) [13].

The roll-off rate is achieved as :

$$\xi = \frac{\alpha_{max} - \alpha_{min}}{f_s - f_c} \quad \ldots\ldots (5)$$

where α_{max} is the highly attenuation point close to passband, α_{min} is 3 dB attenuation point and f_s is the frequency at α_{max}. The relative stopband width ratio (RSB) can be calculated by [13] :

$$RSB = \frac{\text{stopband width}}{\text{cut off frequency}} \quad \ldots\ldots (6)$$

The normalized size of the microstrip filter (NCS) is given by [13]. :

$$\text{NCS} = \frac{\text{Physical size (length} \times \text{width)}}{{\lambda_g}^2} \quad \ldots\ldots (7)$$

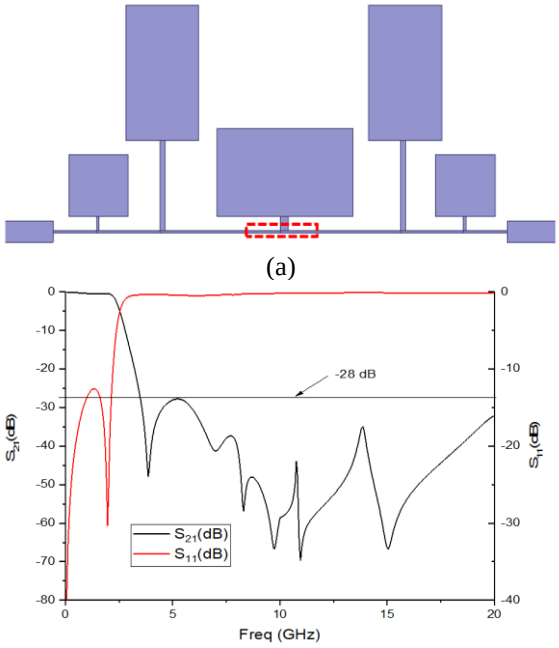

Fig. 6 (a) Top view of the 11th generalized Chebyshev microstrip LPF with DGS (b) Simulation of the frequency response of the 11th generalized Chebyshev microstrip LPF with DGS.

The suppression factor (SF) of the microstrip filter is [13]:

$$\text{SF} = \frac{\text{suppression level in stopband}}{10} \quad \ldots\ldots (8)$$

the architecture factor (AF) is equal to one for two dimensions structure and two for three dimensions. The figure of merit (FOM) is defined as[13]:

$$\text{FOM} = \frac{\text{RSB} \times \xi \times \text{SF}}{\text{NCS} \times \text{AF}} \quad \ldots\ldots (9)$$

Table 3 illustrates the comparison behaviors for the proposed filter with other references in the same techniques. It seems that the suppression factor (SF) is 2.8, which is better than others, and the normalized circuit size (NCS) is smaller than others.

Based on these metrics, the proposed filter outperforms the other references in terms of FOM, indicating its superior performance compared to the other published filters in the same class.

Table 3**:** Comparing the performance of the suggested LPF with several published papers.

References	ξ	*RSB*	SF	NCS	AF	FOM
[5]	40.2	1.60	1.5	0.0117	1	8246
[6]	34	1.07	2	0.1369	1	531.4
[7]	37.2	1.62	1.5	0.0378	1	2391
[8]	100	1.59	1.8	0.032	1	8955
[9]	43	1.65	2	0.02	1	7095
This work	**37.5**	**1.64**	**2.8**	**0.014**	**1**	**12265**

5. CONCLUSION

This paper presents a highly efficient and compact size generalized Chebyshev microstrip LPF using a T-shaped resonator with a slot in the ground layer. The positions of the TZs have been chosen to enhance the rejection level in the stop band of the LPF. Roger RT/Duroid 5880 substrate was used to represent the LPF microstrip. The simulation results show, a cut-off frequency (f_c) of 2 GHz with a wide stopband rejection ranging from 3.4 to 20 GHz. The selectivity of the LPF is about 37.5 dB/GHz, and DGS offers a 28 dB suppression level compared with 18 dB without using DGS. The compact size, wide stop band, and high suppression level make it suitable for applications in 5G communication systems. The performance of the microstrip LPF is evaluated using a FOM and compared to other filters in the same class.

REFERENCES

[1] M. Makimoto and S. Yamashita, “Microwave Resonators and Filters For Wireless Communication: Theory, Design and Application.” p. 162, 2001.

[2] A. H. Al lowaizi and S. W. Luhaib, “A Transmission Zero Position Control for 28 GHz Rectangular Waveguide Cavity Bandpass Filter,” *Al-Rafidain Eng. J.*, vol. 27, no. 1, pp. 81–89, 2022, doi: 10.33899/rengj.2022.132009.1140.

[3] G. Doktoringenieur, A. Balalem, M. Gutachter, I. Abbas, S. O. Prof, and I. M. Leone, “Analysis , Design , Optimization and Realization of Compact High Performance Printed RF Filters,” 2010.

[4] K. Rajasekaran, J. Jayalakshmi, and J. T., “Design and Analysis of Stepped Impedance Microstrip Low Pass Filter Using ADS Simulation Tool for Wireless Applications,” *Int. J. Sci. Res. Publ.*, vol. 3, no. 8, pp. 1–5, 2013.

[5] Y. Jiang, B. Wei, Y. Heng, X. Guo, B. Cao, and L. Jiang, “Compact superconducting lowpass filter with wide stopband,” *Electron. Lett.*, vol. 53, no. 14, pp. 931–933, 2017, doi: 10.1049/el.2017.0429.

[6] A. Boutejdar, M. Challal, and S. El Hani, “Design of new broad stop band (BSB) lowpass filter using compensated capacitor and Π-H-Π DGS resonator for radar applications,” *Prog. Electromagn. Res. M*, vol. 73, no. June, pp. 91–100, 2018, doi: 10.2528/PIERM18062605.

[7] L. F. Shi, Z. Y. Fan, and D. jin Xin, “Miniaturized low-pass filter based on defected ground structure and compensated microstrip line,” *Microw. Opt. Technol. Lett.*, vol. 62, no. 3, pp. 1093–1097, 2020, doi: 10.1002/mop.32144.

[8] T. K. Rekha, P. Abdulla, P. M. Jasmine, and A. R. Anu, “Compact microstrip lowpass filter with high harmonics suppression using defected structures,” *AEU - Int. J. Electron. Commun.*, vol. 115, p. 153032, 2020, doi: 10.1016/j.aeue.2019.153032.

[9] A. Mandal and T. Moyra, “Compact low-pass filter (LPF) with wide harmonic suppression using interdigital capacitor,” *Frequenz*, vol. 77, no. 1–2, pp. 1–8, 2023, doi: 10.1515/freq-2022-0008.

[10] I. C. Hunter, *Theory and Design of Microwave Filters (IEE Electromagnetic Waves Series)*. 2001. [Online]. Available: http://gen.lib.rus.ec/book/index.php?md5=CA64BCAB5E445FB256D3D019D2F6A803

[11] D. Ibrahim, “Design and Optimization of Butterworth and Elliptic Band Pass Filters in 5G Application,” *Al-Rafidain Eng. J.*, vol. 27, no. 2, pp. 68–81, 2022, doi: 10.33899/rengj.2022.132518.1146.

[12] J. Hong and M. J. Lancaster, *Microstrip Filters for RF / Microwave*, vol. 7. 2001.

[13] M. Hayati, M. Validi, F. Shama, and M. Ekhteraei, “Compact microstrip low-pass filter with wide stop-band using P-shaped resonator,” *J. Microwaves, Optoelectron. Electromagn. Appl.*, vol. 15, no. 4, pp. 309–318, 2016, doi: 10.1590/2179-10742016v15i4633.

تصميم وتصغير مرشح تمرير منخفض ذو الشريحة الرقيقة ذات توقف عالي الدعم باستخدام الهيكل الأرضي المعيب في الفتحة لتطبيقات الجيل الخامس

اشرف خالد عزيز الحسين ashraf.21enp13@student.uomosul.edu.iq

سعد وسمي عصمان لهيب s.w.o.luhaib@uomosul.edu.iq

قسم الهندسة الكهربائية, كلية الهندسة, جامعة الموصل, الموصل, العراق

تاريخ الاستلام: 11 ديسمبر 2023 استلم بصيغته المنقحة: 30 يناير 2024 تاريخ القبول: 18 فبراير 2024

الملخص

هذا البحث، يتم عرض مرشح تمرير منخفض ذو شريط إيقاف عالي القمع. تم تنفيذ مرنانات المرشح المقترح باستخدام شريط صغير على شكل حرف T. *تتكون مرنانات المرشح من ثلاثة أجزاء رئيسية. تم استخدام جزء من الرنانات لتحسين رفض المرشح في منطقة التوقف والجزء الثاني لزيادة انتقائية المرشح، والجزء الأخير استخدم لتحقيق التوازن بين المنطقتين. تم تصميم مرشح* microstrip LPF *على ركيزة* Roger RT/Duroid 5880 *بـ* εr=2.2*، وسمك 0.381 مم. تمت محاكاة الترتيب الحادي عشر المعمم* Chebyshev LPF *باستخدام برنامج* HFSS. *وكانت نتائج المحاكاة كما يلي: 2 جيجا هرتز لتردد القطع، وخسارة إدخال قدرها 0,55 ديسيبل عند خسارة إرجاع تبلغ حوالي 20 ديسيبل، ومدى واسع من كبت نطاق التوقف تحت مستوى 28 ديسيبل من التردد 3,4 جيجا هرتز إلى 20 جيجا هرتز. كانت انتقائية* LPF *حوالي 37.5 ديسيبل / جيجا هرتز وتم تقديم مرشح صغير الحجم وصغير الحجم بـ 0.014* µ g. *المرشح مطابق للمواصفات المطلوبة لمرشحات الجيل الخامس في أنظمة الاتصالات اللاسلكية.*

الكلمات الداله :

مرشح الامرار الواطىء، الشريحة الرقيقة، الصد العالي،التركيب معيوب الارضي.